Interplay between non-collinear magnetism and nanoscale structural properties in epitaxial Fe-based ultrathin films

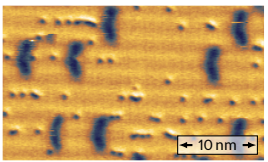

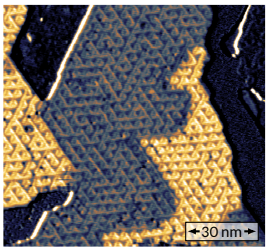

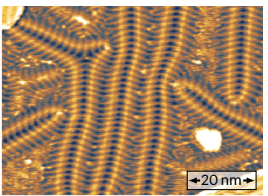

Magnetic ultrathin films

Magnetic ultrathin films

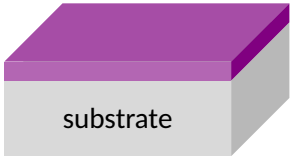

Sputter deposition

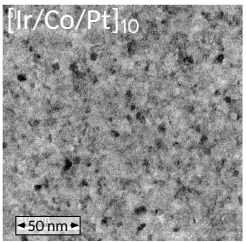

S. McVitie *et al.* *Scientific Reports* 8 (2018), 5703

Magnetic ultrathin films

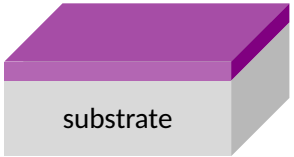

↕ a few nm

Evaporation

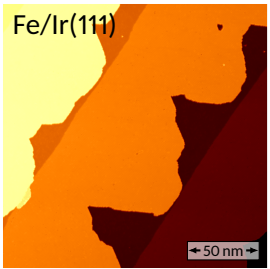

Sputter deposition

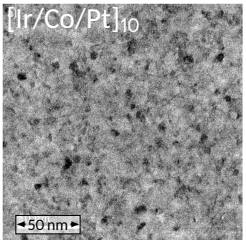

S. McVitie *et al.* *Scientific Reports* 8 (2018), 5703

Magnetic ultrathin films

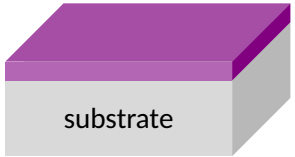

Evaporation

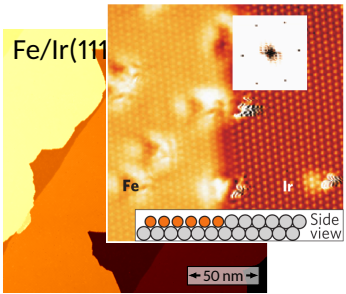

S. Heinze *et al.* *Nat Phys* 7 (2011), 713–718

Sputter deposition

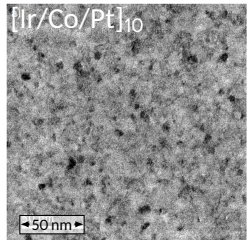

S. McVitie *et al.* *Scientific Reports* 8 (2018), 5703

Magnetic ultrathin films

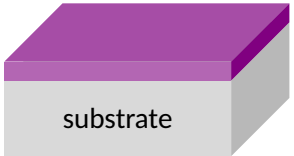

Evaporation

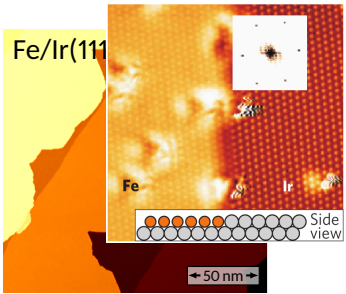

S. Heinze *et al.* *Nat Phys* 7 (2011), 713–718

Strain relief effects

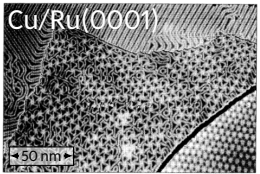

C. Günther *et al.* *Phys. Rev. Lett.* 74 (1995), 754–757

Sputter deposition

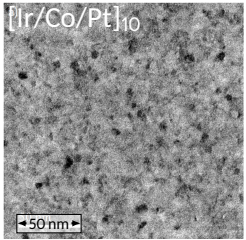

S. McVitie *et al.* *Scientific Reports* 8 (2018), 5703

Spin-polarized Scanning Tunneling Microscopy (SP-STM)

Tunneling MagnetoResistance

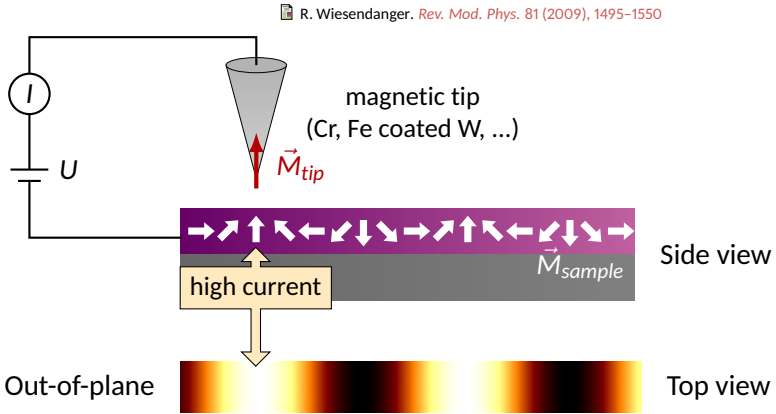

$$I = I_0 \left(1 + P_{sample} P_{tip} \cos\left(\vec{M}_{sample}, \vec{M}_{tip}\right)\right)$$

Spin-polarized Scanning Tunneling Microscopy (SP-STM)

Tunneling MagnetoResistance

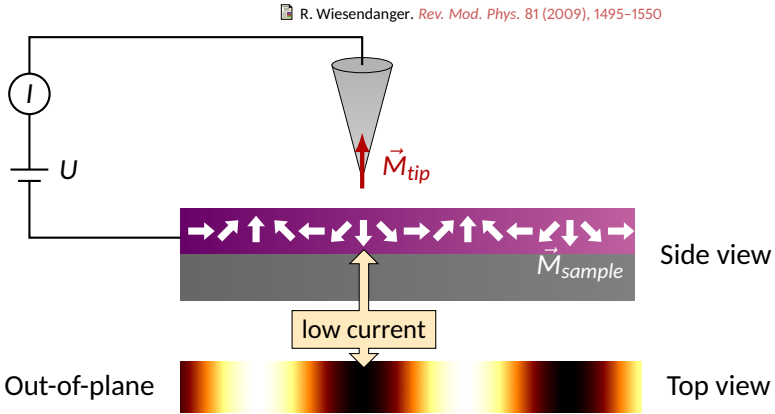

$$I = I_0 \left(1 + P_{sample} P_{tip} \cos\left(\vec{M}_{sample}, \vec{M}_{tip}\right)\right)$$

Spin-polarized Scanning Tunneling Microscopy (SP-STM)

Tunneling MagnetoResistance

R. Wiesendanger. *Rev. Mod. Phys.* 81 (2009), 1495–1550

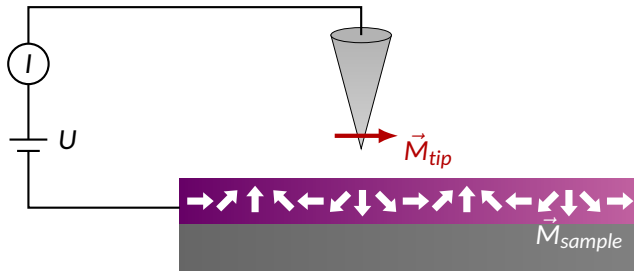

Side view

Out-of-plane

Top view

In-plane

Top view

Spin-polarized Scanning Tunneling Microscopy (SP-STM)

Tunneling MagnetoResistance

R. Wiesendanger. *Rev. Mod. Phys.* 81 (2009), 1495–1550

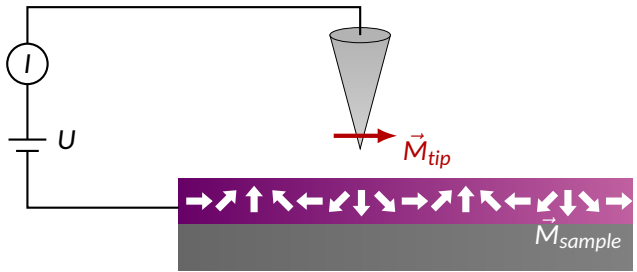

Side view

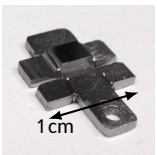

Top view

Top view

Competition between the different magnetic contributions

Exchange coupling

$$\mathcal{E}_{\text{exch}} = \sum_{i \neq j} J_{ij}\, \vec{m}_i \cdot \vec{m}_j$$

Competition between the different magnetic contributions

Exchange coupling

$$\mathcal{E}_{\text{exch}} = \sum_{i \neq j} J_{ij}\, \vec{m}_i \cdot \vec{m}_j$$

Effective anisotropy

$$\mathcal{E}_{\text{ani}} = \sum_{i} K_i\, (\vec{m}_i \cdot \hat{e}_z)^2$$

Competition between the different magnetic contributions

Exchange coupling

$$\mathcal{E}_{\text{exch}} = \sum_{i \neq j} J_{ij}\, \vec{m}_i \cdot \vec{m}_j$$

Effective anisotropy

$$\mathcal{E}_{\text{ani}} = \sum_{i} K_i \, (\vec{m}_i \cdot \hat{e}_z)^2$$

Dzyaloshinkii-Moriya interaction (DMI)

$$\mathcal{E}_{\text{DM}} = \sum_{ij} \vec{D}_{ij} \cdot (\vec{m}_i \times \vec{m}_j)$$

Competition between the different magnetic contributions

Exchange coupling

$$\mathcal{E}_{\text{exch}} = \sum_{i \neq j} J_{ij}\, \vec{m}_i \cdot \vec{m}_j$$

Effective anisotropy

$$\mathcal{E}_{\text{ani}} = \sum_{i} K_i \left(\vec{m}_i \cdot \hat{e}_z\right)^2$$

Dzyaloshinkii-Moriya interaction (DMI)

$$\mathcal{E}_{\text{DM}} = \sum_{ij} \vec{D}_{ij} \cdot \left(\vec{m}_i \times \vec{m}_j\right)$$

Higher-order interactions

Biquadratic interaction, four-spin interaction, ...

Competition between the different magnetic contributions

Exchange coupling

$$\mathcal{E}_{\text{exch}} = \sum_{i \neq j} J_{ij}\, \vec{m}_i \cdot \vec{m}_j$$

Effective anisotropy

$$\mathcal{E}_{\text{ani}} = \sum_{i} K_i \left(\vec{m}_i \cdot \hat{e}_z\right)^2$$

Dzyaloshinkii-Moriya interaction (DMI)

$$\mathcal{E}_{\text{DM}} = \sum_{ij} \vec{D}_{ij} \cdot \left(\vec{m}_i \times \vec{m}_j\right)$$

Higher-order interactions

Biquadratic interaction, four-spin interaction, …

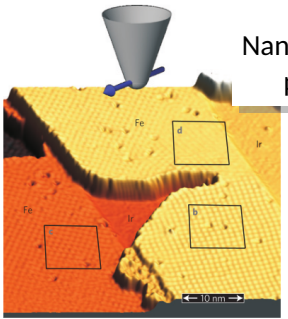

Fe/Ir(111)
Nanoskyrmion lattice
period $\sim$ 1 nm

D = −1.8 meV
per atom

S. Heinze *et al.* *Nat Phys* 7 (2011), 713–718

Overview of the studied systems

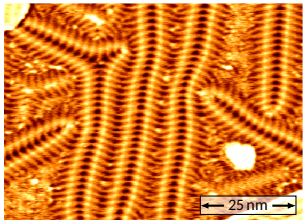

Fe/Fe/Ir(111)

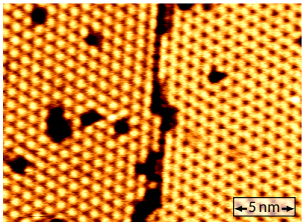

H-Fe/Ir(111)

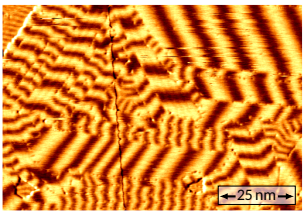

Fe/Fe/Fe/Ir(111)

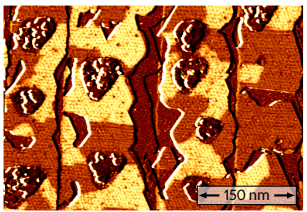

Ni/Fe/Ir(111)

Overview of the studied systems

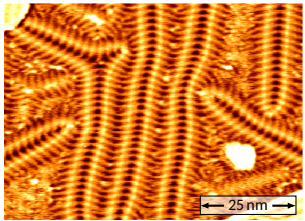

Fe/Fe/Ir(111)

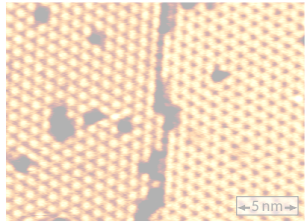

H-Fe/Ir(111)

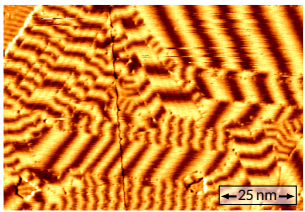

Fe/Fe/Fe/Ir(111)

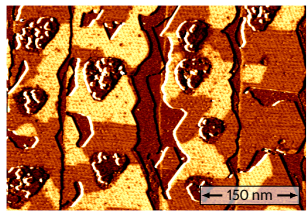

Ni/Fe/Ir(111)

Triangular pattern in Ni/Fe/Ir(111)

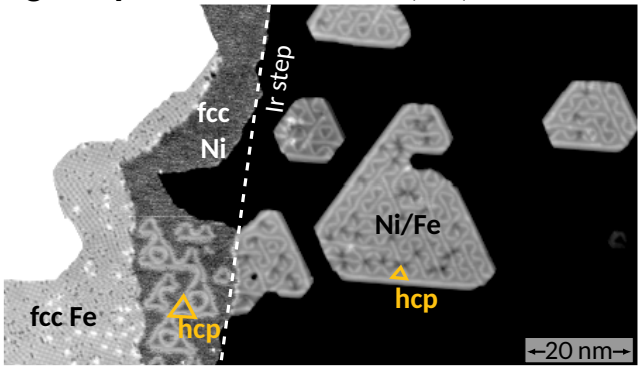

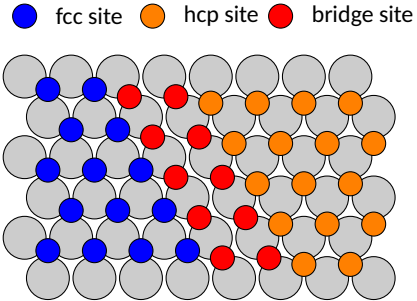

D. Iaia *et al.* *Phys. Rev. B* 93 (2016), 134409

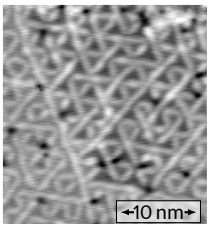

- Alternating triangular fcc and hcp areas
- Separated by bridge lines

Triangular pattern in Ni/Fe/Ir(111)

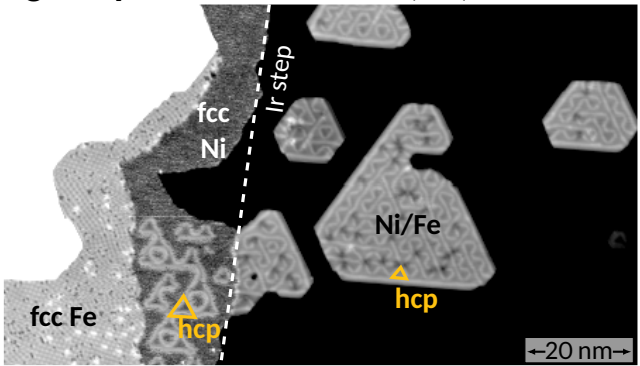

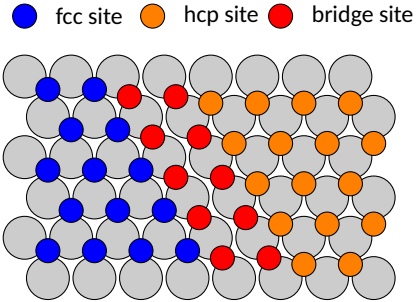

D. Iaia *et al.* *Phys. Rev. B* 93 (2016), 134409

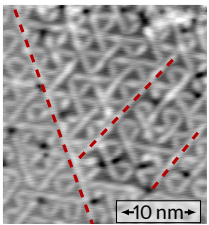

- Alternating triangular fcc and hcp areas
- Separated by bridge lines
- Some of the bridge lines are very long and influence the magnetic state

Strong pinning of the domain walls to the bridge lines

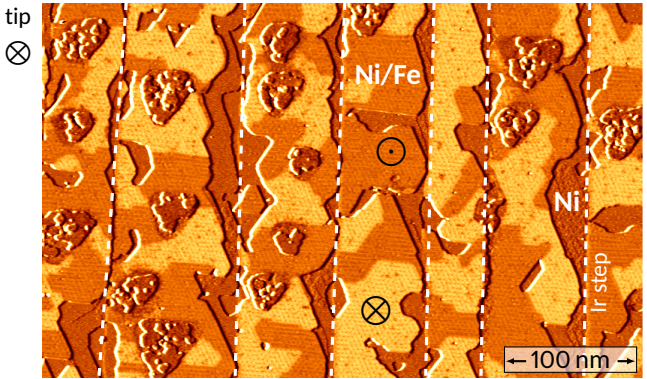

100 mV, 1 nA, 4 K, 0 T

- Out-of-plane ferromagnetic domains

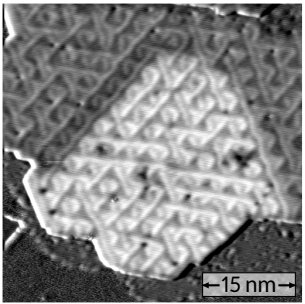

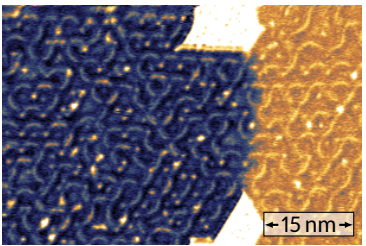

Co/Pt(111), measured by M. Perini

Strong pinning of the domain walls to the bridge lines

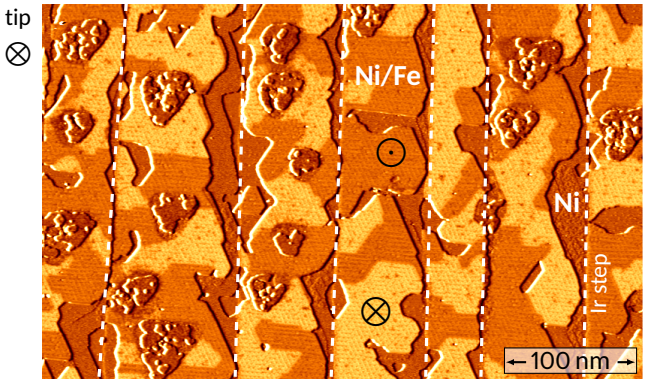

100 mV, 1 nA, 4 K, 0 T

- Out-of-plane ferromagnetic domains
- Domain walls pinned at the long bridge lines
- Modification of exchange, DMI or anisotropy at the lines, making the walls energetically more favorable

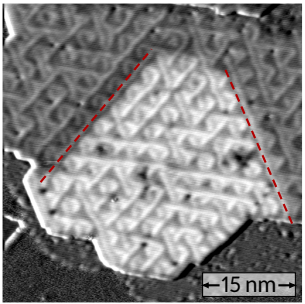

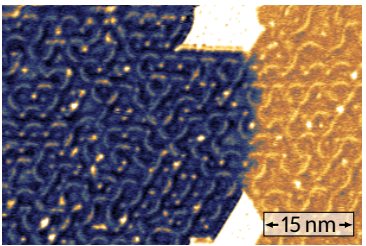

Co/Pt(111), measured by M. Perini

Overview of the studied systems

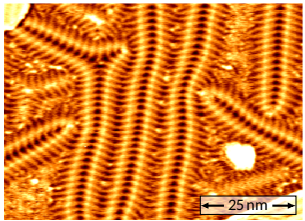

Fe/Fe/Ir(111)

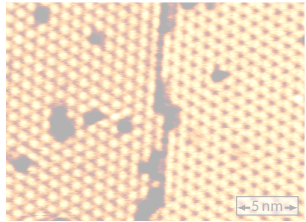

H-Fe/Ir(111)

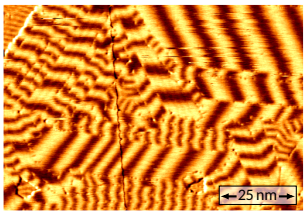

Fe/Fe/Fe/Ir(111)

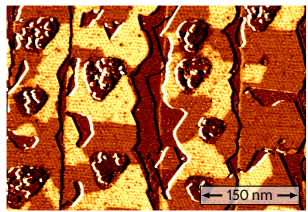

Ni/Fe/Ir(111)

The Fe double layer on Ir(111)

Bulk Fe: bcc

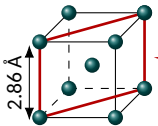

bcc(110) nearest neighbor distance: $a = 2.47$ Å

Lattice mismatch!

Bulk Ir: fcc

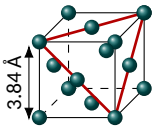

fcc(111) nearest neighbor distance: $a = 2.72$ Å

The Fe double layer on Ir(111)

Bulk Fe: bcc

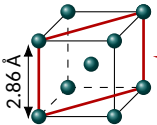

bcc(110) nearest neighbor distance: $a = 2.47$ Å

Bulk Ir: fcc

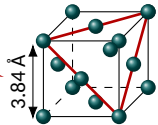

fcc(111) nearest neighbor distance: $a = 2.72$ Å

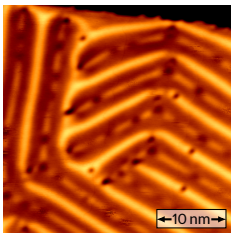

200 mV, 1 nA, 5 K, 0 T

P.-J. Hsu, A. Finco *et al.* *Phys. Rev. Lett.* 116 (2016), 017201

The Fe double layer on Ir(111)

Bulk Fe: bcc

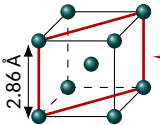

bcc(110) nearest neighbor distance: $a = 2.47$ Å

Lattice mismatch!

Bulk Ir: fcc

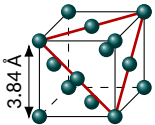

fcc(111) nearest neighbor distance: $a = 2.72$ Å

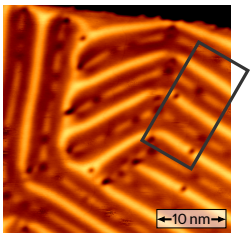

200 mV, 1 nA, 5 K, 0 T

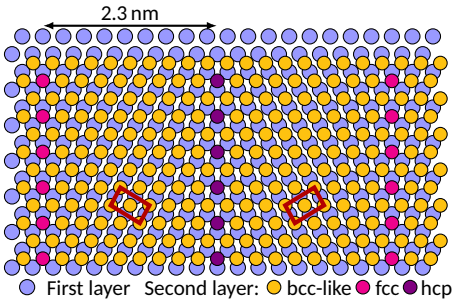

P.-J. Hsu, A. Finco *et al.* *Phys. Rev. Lett.* 116 (2016), 017201

The Fe double layer on Ir(111)

Bulk Fe: bcc

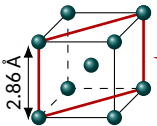

bcc(110) nearest neighbor distance: $a = 2.47$ Å

Lattice mismatch!

Bulk Ir: fcc

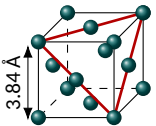

fcc(111) nearest neighbor distance: $a = 2.72$ Å

- Spin spirals
- Guided propagation along the dislocation lines
- Period ~ 1.5 nm
- No change up to 9 T

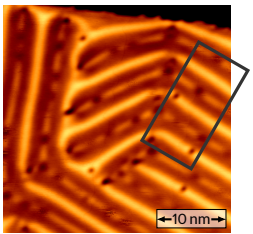

200 mV, 1 nA, 5 K, 0 T

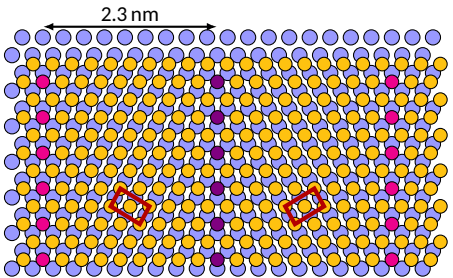

tip

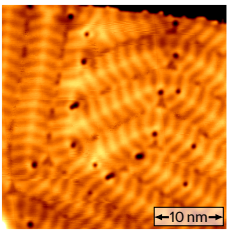

1 V, 2 nA, 5 K, 4 T

P.-J. Hsu, A. Finco *et al.* *Phys. Rev. Lett.* 116 (2016), 017201

The Fe triple layer on Ir(111)

Constant current map

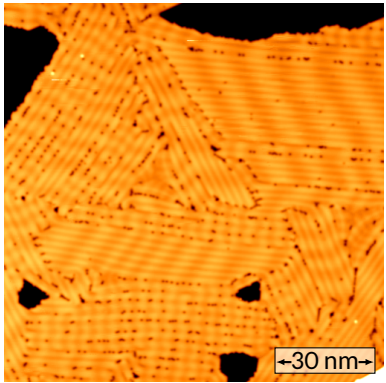

−700 mV, 1 nA, 8 K, 0 T, Cr bulk tip

The Fe triple layer on Ir(111)

Constant current map

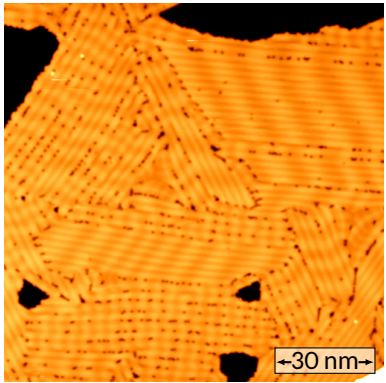

−700 mV, 1 nA, 8 K, 0 T, Cr bulk tip

Differential conductance map

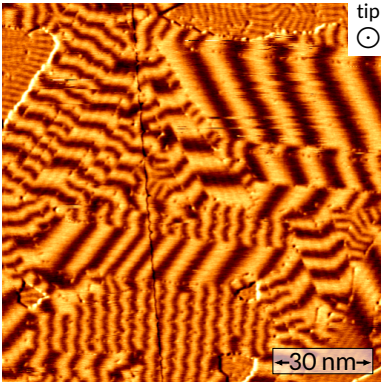

−700 mV, 1 nA, 8 K, 0 T, Cr bulk tip

The Fe triple layer on Ir(111)

Constant current map

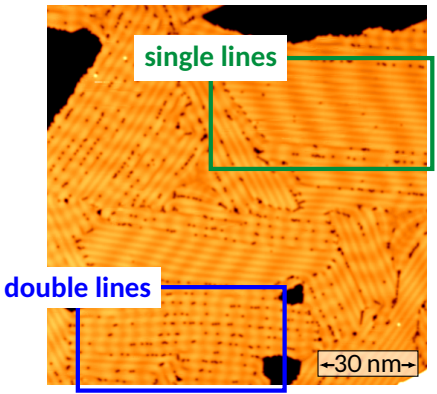

−700 mV, 1 nA, 8 K, 0 T, Cr bulk tip

- Same appearance at any voltage, positive or negative
- Line spacing: 1.8 to 2.2 nm
- Spin spiral period: 5 to 10 nm
- Straight but canted spiral wavefront

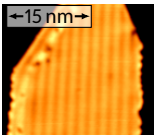

+200 mV

- Double line feature only at positive voltage
- Line spacing: 2.2 to 2.8 nm
- Spin spiral period: 3 to 4 nm
- Zigzag spiral wavefront

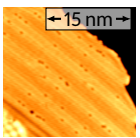

+200 mV

A. Finco *et al.* *Phys. Rev. B* 94 (2016), 214402

Double lines, atomic structure model

A. Finco *et al.* *Phys. Rev. B* 94 (2016), 214402

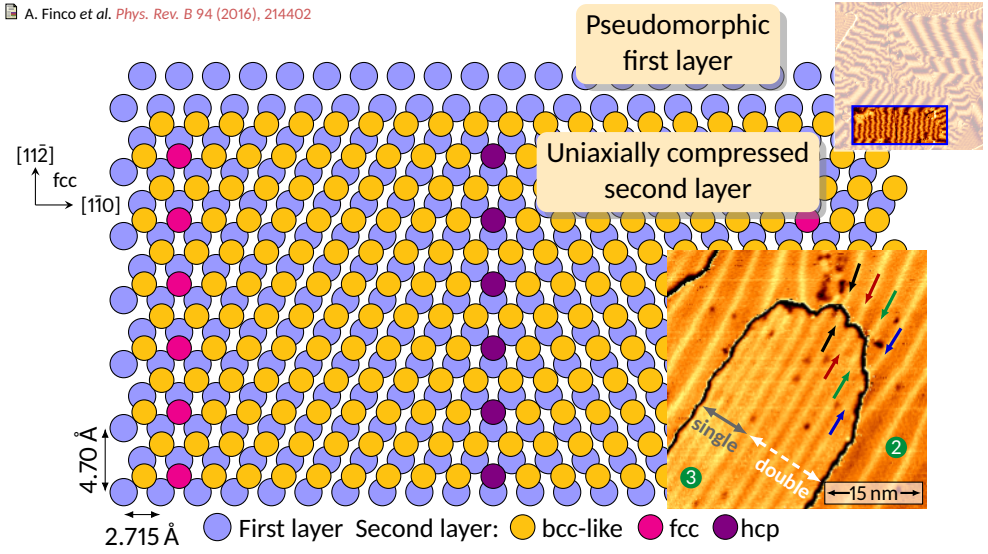

Double lines, atomic structure model

A. Finco *et al.* *Phys. Rev. B* 94 (2016), 214402

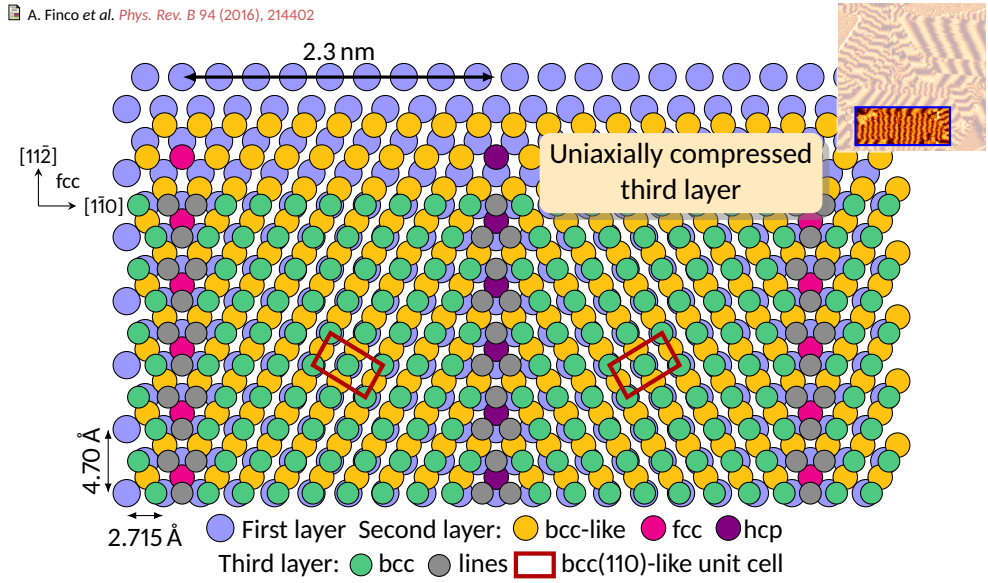

Single lines, atomic structure model

A. Finco *et al.* *Phys. Rev. B* 94 (2016), 214402

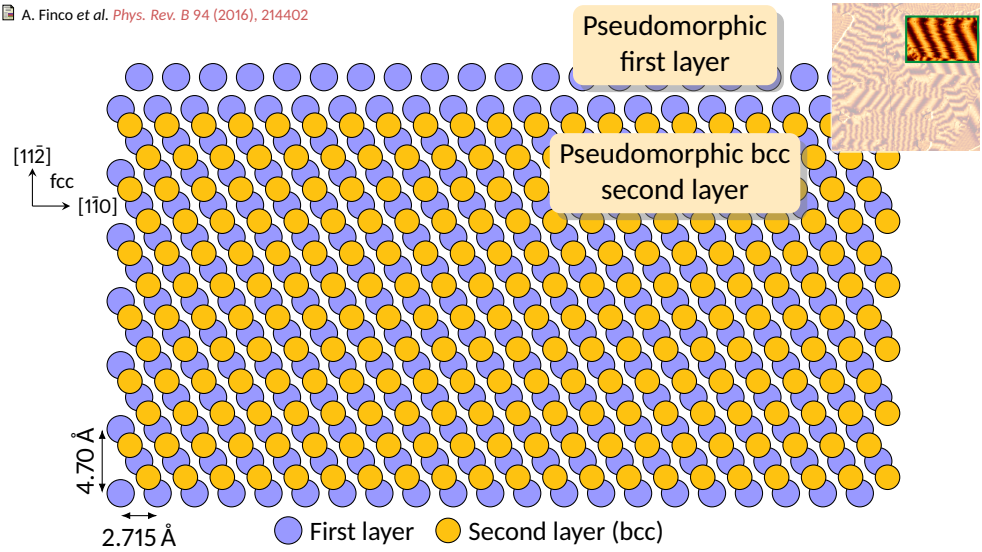

Single lines, atomic structure model

A. Finco *et al.* *Phys. Rev. B* 94 (2016), 214402

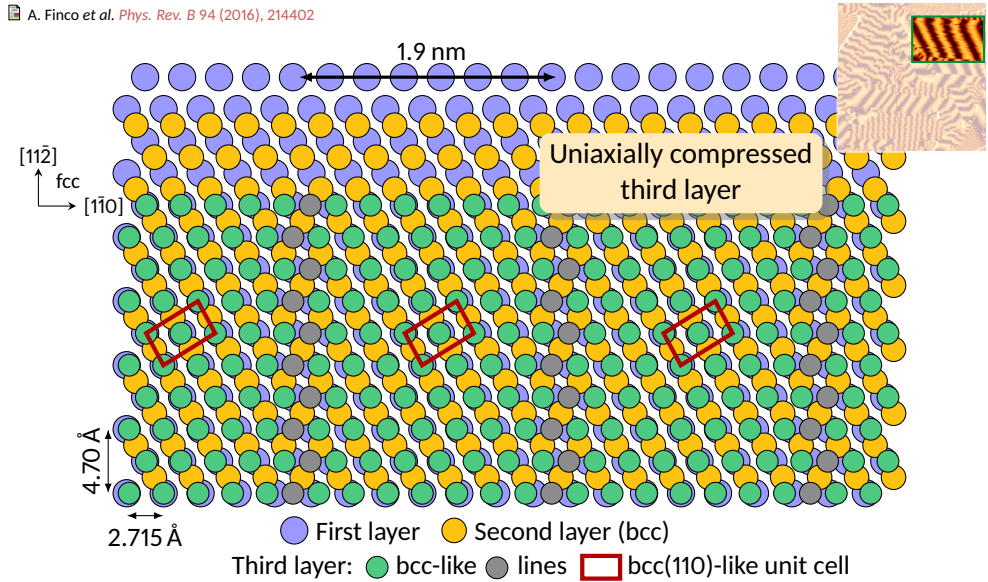

Varying spin spiral period

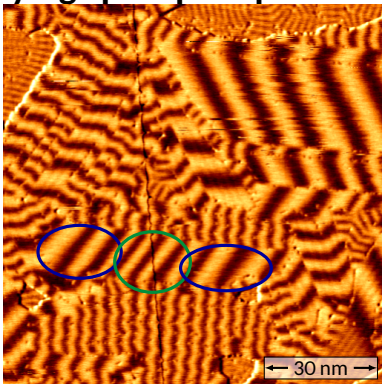

Magnetic period:

7.5 nm

4.9 nm

Dislocation lines spacing:

1.85 nm

2.1 nm

Varying spin spiral period

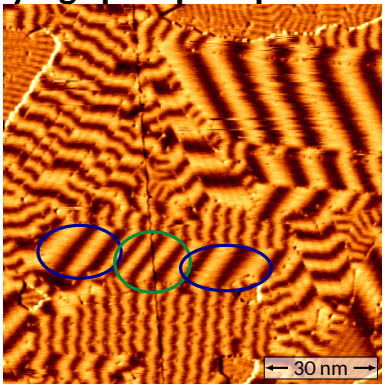

Magnetic period:

7.5 nm

4.9 nm

Dislocation lines spacing:

1.85 nm

2.1 nm

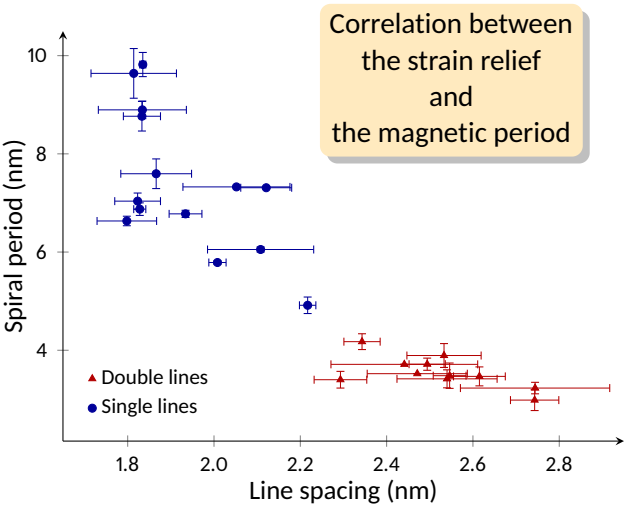

A. Finco *et al.* *Phys. Rev. B* 94 (2016), 214402

Micromagnetic 1D model

A. Bogdanov *et al.* *J. Magn. Magn. Mater.* 138 (1994), 255–269

1D model

$$\mathcal{E} = A\left(\frac{\mathrm{d}\vec{m}}{\mathrm{d}x}\right)^2 + D\left(m_z\frac{\mathrm{d}m_x}{\mathrm{d}x} - m_x\frac{\mathrm{d}m_z}{\mathrm{d}x}\right) - K_{\mathrm{eff}}m_z^2$$

exchange coupling — DMI — effective anisotropy

Micromagnetic 1D model

A. Bogdanov *et al.* *J. Magn. Magn. Mater.* 138 (1994), 255–269

1D model

$$\mathcal{E} = A\left(\frac{\mathrm{d}\vec{m}}{\mathrm{d}x}\right)^2 + D\left(m_z\frac{\mathrm{d}m_x}{\mathrm{d}x} - m_x\frac{\mathrm{d}m_z}{\mathrm{d}x}\right) - K_{\mathrm{eff}}m_z^2$$

exchange coupling

DMI

effective anisotropy

comes from the interface

$|D| = 2.8\,\mathrm{mJ\,m^{-2}}$

Micromagnetic 1D model

A. Bogdanov *et al.* *J. Magn. Magn. Mater.* 138 (1994), 255–269

1D model

$$\mathcal{E} = A\left(\frac{\mathrm{d}\vec{m}}{\mathrm{d}x}\right)^2 + D\left(m_z\frac{\mathrm{d}m_x}{\mathrm{d}x} - m_x\frac{\mathrm{d}m_z}{\mathrm{d}x}\right) - K_{\mathrm{eff}}m_z^2$$

exchange coupling

DMI

effective anisotropy

comes from the interface

$|D| = 2.8\,\mathrm{mJ\,m^{-2}}$

Magnetic signal

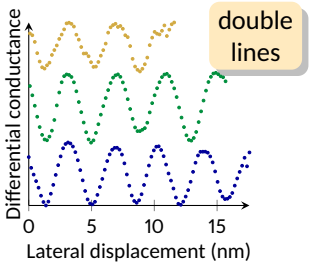

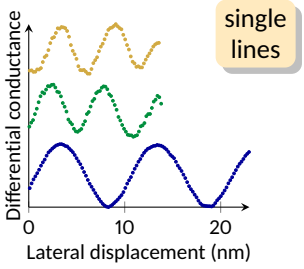

Micromagnetic 1D model

A. Bogdanov *et al.* *J. Magn. Magn. Mater.* 138 (1994), 255–269

1D model

$$\mathcal{E} = A\left(\frac{\mathrm{d}\vec{m}}{\mathrm{d}x}\right)^2 + D\left(m_z\frac{\mathrm{d}m_x}{\mathrm{d}x} - m_x\frac{\mathrm{d}m_z}{\mathrm{d}x}\right) - K_{\mathrm{eff}}m_z^2$$

exchange coupling

DMI

comes from the interface

$|D| = 2.8\,\mathrm{mJ\,m^{-2}}$

effective anisotropy

negligible

$K_{\mathrm{eff}} = 0$

$\lambda = 4\pi\frac{A}{|D|}$

Magnetic signal

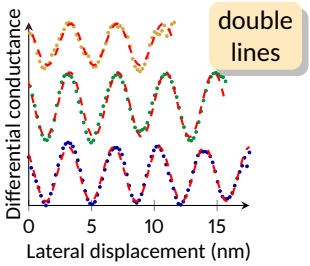

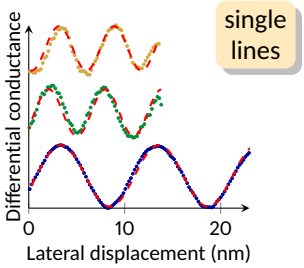

Micromagnetic 1D model

A. Bogdanov *et al.* *J. Magn. Magn. Mater.* 138 (1994), 255–269

1D model

$$\mathcal{E} = A\left(\frac{d\vec{m}}{dx}\right)^2 + D\left(m_z\frac{dm_x}{dx} - m_x\frac{dm_z}{dx}\right) - K_{\text{eff}}m_z^2$$

- exchange coupling → affected by the non-uniform strain relief
- DMI → comes from the interface $|D| = 2.8\,\text{mJ m}^{-2}$
- effective anisotropy → negligible $K_{\text{eff}} = 0$ → $\lambda = 4\pi\frac{A}{|D|}$

Magnetic signal

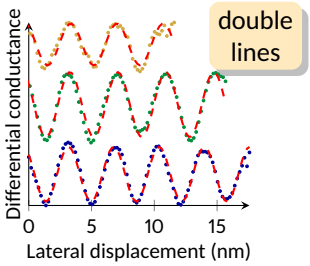

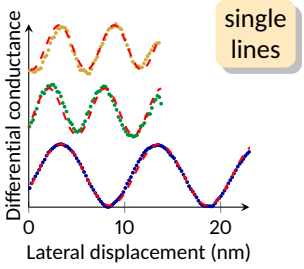

Micromagnetic 1D model

A. Bogdanov *et al.* *J. Magn. Magn. Mater.* 138 (1994), 255–269

1D model

$$\mathcal{E} = A\left(\frac{\mathrm{d}\vec{m}}{\mathrm{d}x}\right)^2 + D\left(m_z\frac{\mathrm{d}m_x}{\mathrm{d}x} - m_x\frac{\mathrm{d}m_z}{\mathrm{d}x}\right) - K_{\mathrm{eff}}m_z^2$$

exchange coupling	DMI	effective anisotropy
⬇	⬇	⬇
affected by the non-uniform strain relief	comes from the interface $\lvert D\rvert = 2.8\,\mathrm{mJ\,m^{-2}}$	negligible $K_{\mathrm{eff}} = 0$
		⬇
		$\lambda = 4\pi\frac{A}{\lvert D\rvert}$

$3\,\mathrm{nm} \leqslant \lambda \leqslant 10\,\mathrm{nm}$

⬍

$0.6\,\mathrm{pJ\,m^{-1}} \leqslant A \leqslant 2.2\,\mathrm{pJ\,m^{-1}}$

Magnetic signal

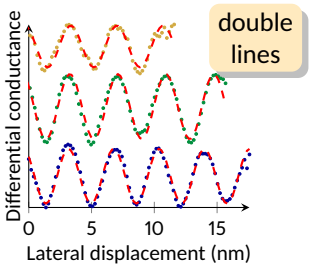

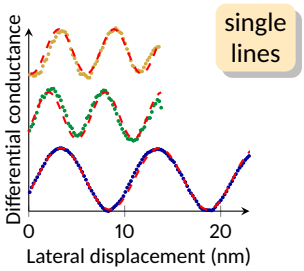

Effect of an external magnetic field

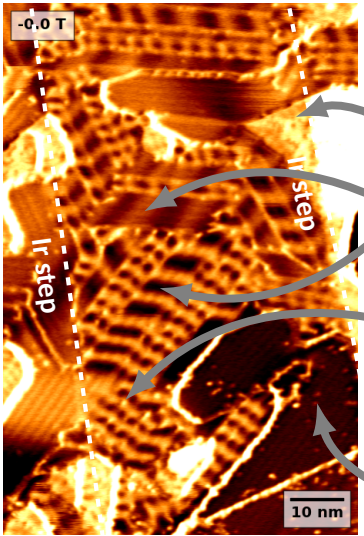

Double layer

Triple layer
single lines

Triple layer
double lines

Quadruple
layer

−500 mV, 1 nA, 4 K

Effect of an external magnetic field

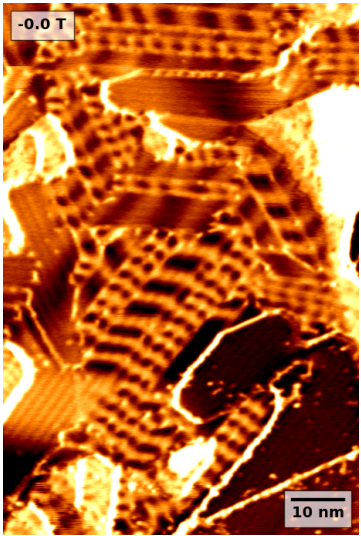

Effect of an external magnetic field

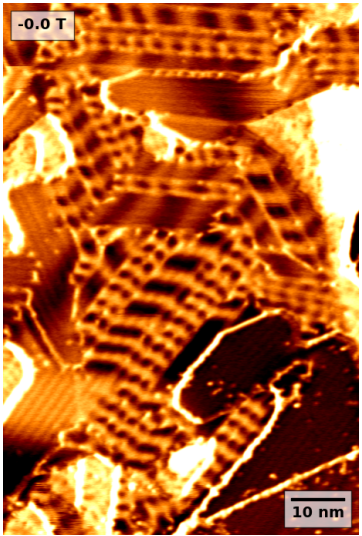

Quadruple layer:

- Ferromagnetic state reached at 0.5 T

Triple layer, single lines:

- Dark stripes get thinner, move and disappear
- Ferromagnetic state reached at 2 T

Triple layer, double lines:

- Spirals split up in individual magnetic objects
- Aligned on the dislocation lines
- Isolated around 3 T
- Ferromagnetic state reached around 4 T

Magnetic skyrmions

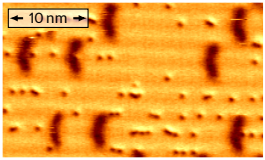

−700 mV, 1 nA, 8 K, 2.5 T

Magnetic skyrmions

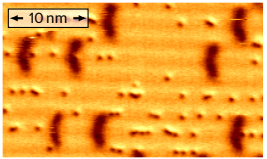

−700 mV, 1 nA, 8 K, 2.5 T

Skyrmions

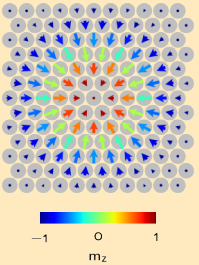

- Localized magnetic configuration
- Topological charge
- Stabilized by the DMI

Magnetic skyrmions

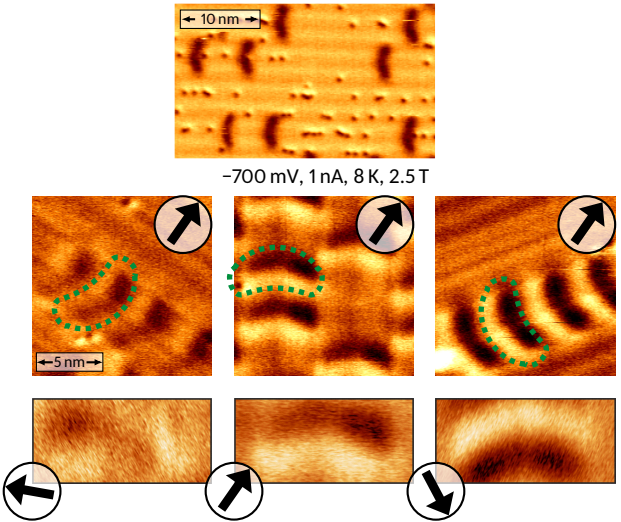

Skyrmions

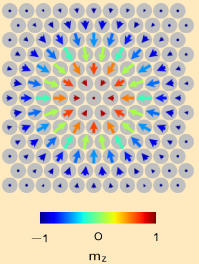

- Localized magnetic configuration
- Topological charge
- Stabilized by the DMI

P.-J. Hsu, A. Finco *et al.* *Nat. Nanotechnol.* 12 (2017), 123–126

Magnetic skyrmions

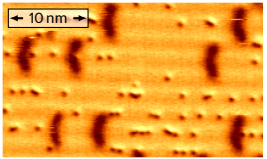

−700 mV, 1 nA, 8 K, 2.5 T

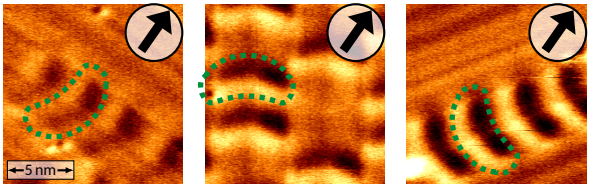

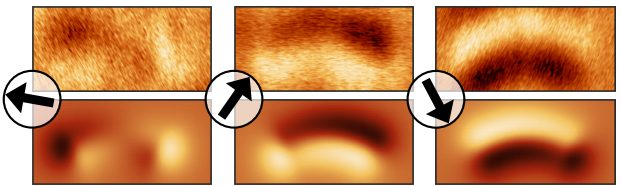

Skyrmions

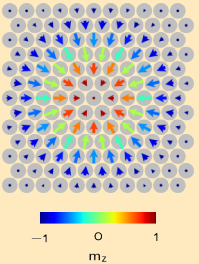

- Localized magnetic configuration
- Topological charge
- Stabilized by the DMI

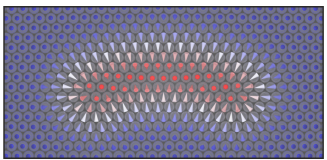

P.-J. Hsu, A. Finco *et al.* *Nat. Nanotechnol.* 12 (2017), 123–126

Manipulation of the skyrmions using a STM tip

Pd/Fe/Ir(111)

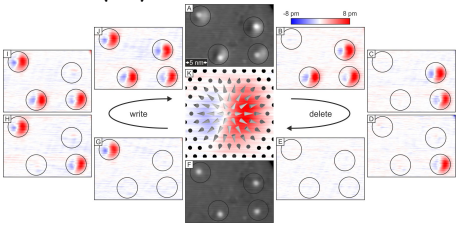

N. Romming *et al.* *Science* 341 (2013), 636–639

Manipulation of the skyrmions using a STM tip

Pd/Fe/Ir(111)

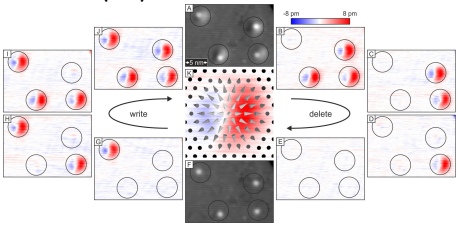

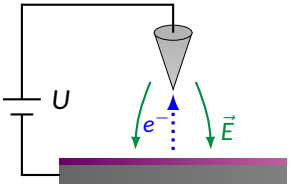

N. Romming *et al.* *Science* 341 (2013), 636–639

Manipulation of the skyrmions using a STM tip

Pd/Fe/Ir(111)

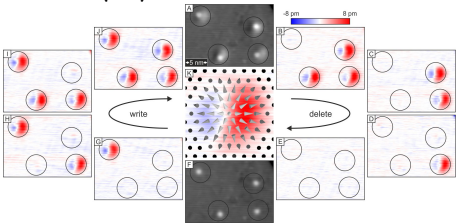

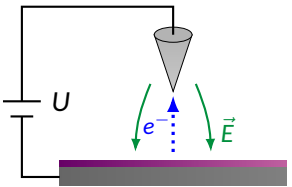

N. Romming *et al.* *Science* 341 (2013), 636–639

Deleting, ramp to −3 V

Imaging: 300 mV, 0.5 nA, 8 K, 2.5 T, Cr bulk tip

Manipulation of the skyrmions using a STM tip

Pd/Fe/Ir(111)

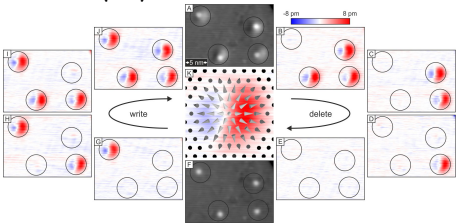

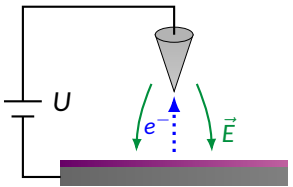

N. Romming *et al.* *Science* 341 (2013), 636–639

Deleting, ramp to −3 V

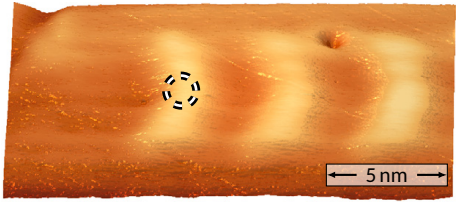

Imaging: 300 mV, 0.5 nA, 8 K, 2.5 T, Cr bulk tip

Manipulation of the skyrmions using a STM tip

Pd/Fe/Ir(111)

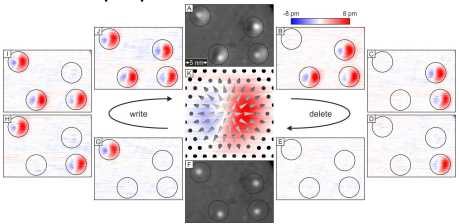

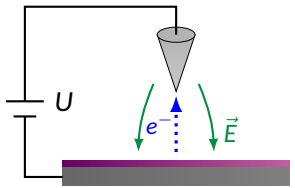

N. Romming *et al.* *Science* 341 (2013), 636–639

Deleting, ramp to −3 V

Imaging: 300 mV, 0.5 nA, 8 K, 2.5 T, Cr bulk tip

Manipulation of the skyrmions using a STM tip

Pd/Fe/Ir(111)

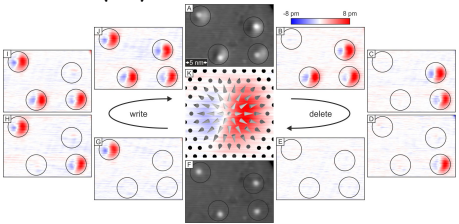

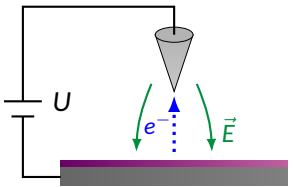

N. Romming *et al.* *Science* 341 (2013), 636–639

Deleting, ramp to −3 V

Imaging: 300 mV, 0.5 nA, 8 K, 2.5 T, Cr bulk tip

Manipulation of the skyrmions using a STM tip

Pd/Fe/Ir(111)

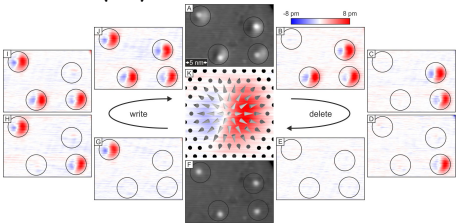

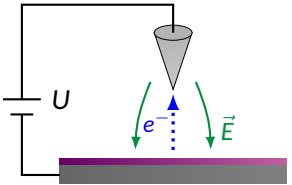

N. Romming *et al.* *Science* 341 (2013), 636–639

Deleting, ramp to −3 V

Writing, ramp to 3 V

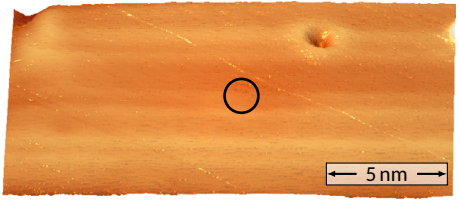

Imaging: 300 mV, 0.5 nA, 8 K, 2.5 T, Cr bulk tip

Manipulation of the skyrmions using a STM tip

Pd/Fe/Ir(111)

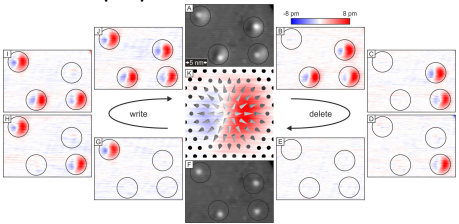

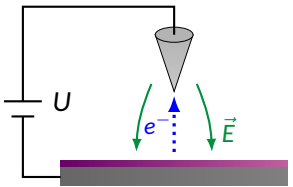

N. Romming *et al.* *Science* 341 (2013), 636–639

Deleting, ramp to −3 V

Writing, ramp to 3 V

Imaging: 300 mV, 0.5 nA, 8 K, 2.5 T, Cr bulk tip

Manipulation of the skyrmions using a STM tip

Pd/Fe/Ir(111)

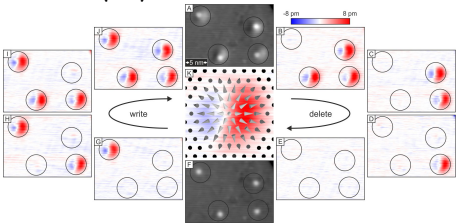

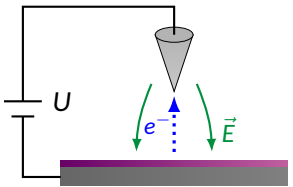

N. Romming *et al.* *Science* 341 (2013), 636–639

Deleting, ramp to −3 V

Writing, ramp to 3 V

Imaging: 300 mV, 0.5 nA, 8 K, 2.5 T, Cr bulk tip

Switching with a non-magnetic tip

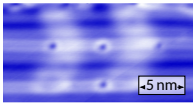

200 mV, 1 nA, 8 K, −1.85 T, W tip

Switching with a non-magnetic tip

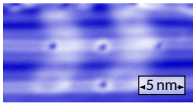

200 mV, 1 nA, 8 K, −1.85 T, W tip

Non-CollinearMagnetoResistance

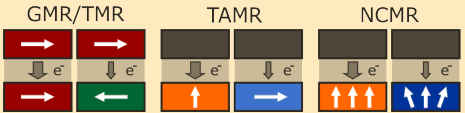

C. Hanneken *et al.* *Nat. Nanotechnol.* 10 (2015), 1039–1042

Switching with a non-magnetic tip

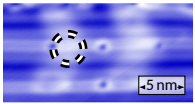

200 mV, 1 nA, 8 K, −1.85 T, W tip

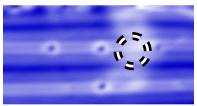

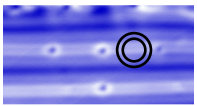

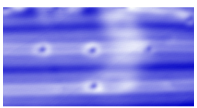

Non-CollinearMagnetoResistance

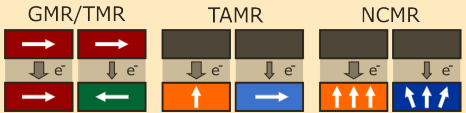

C. Hanneken *et al.* *Nat. Nanotechnol.* 10 (2015), 1039–1042

Switching with a non-magnetic tip

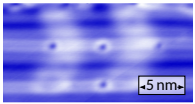

200 mV, 1 nA, 8 K, −1.85 T, W tip

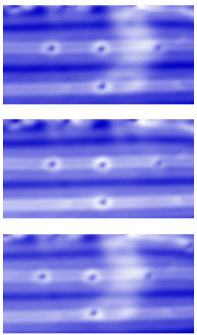

Non-CollinearMagnetoResistance

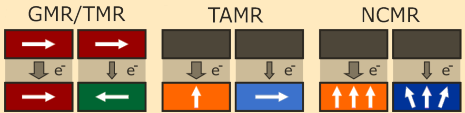

C. Hanneken *et al.* *Nat. Nanotechnol.* 10 (2015), 1039–1042

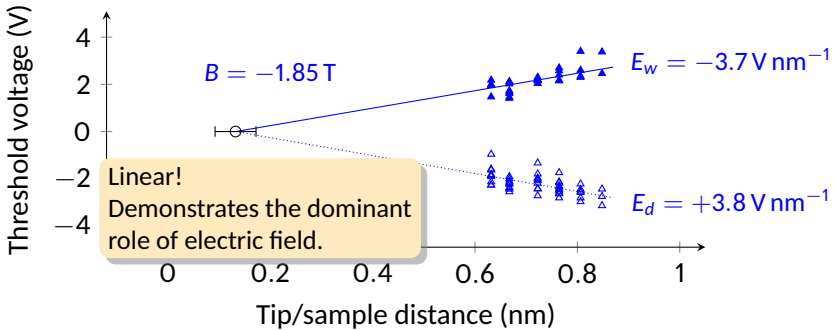

Linear!
Demonstrates the dominant role of electric field.

P.-J. Hsu, A. Finco *et al.* *Nat. Nanotechnol.* 12 (2017), 123–126

Improved thermal stability

Fe monolayer on Ir(111)

Nanoskyrmion lattice visible until 28 K

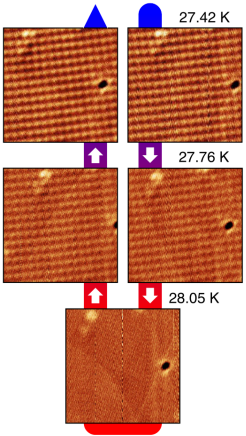

A. Sonntag *et al.* *Phys. Rev. Lett.* 113 (2014), 077202

Improved thermal stability

Fe monolayer on Ir(111)

Nanoskyrmion lattice visible until 28 K

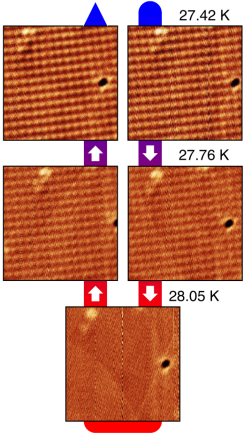

A. Sonntag *et al.* *Phys. Rev. Lett.* 113 (2014), 077202

Fe double layer on Ir(111)

The spin spirals disappear between 150 and 200 K

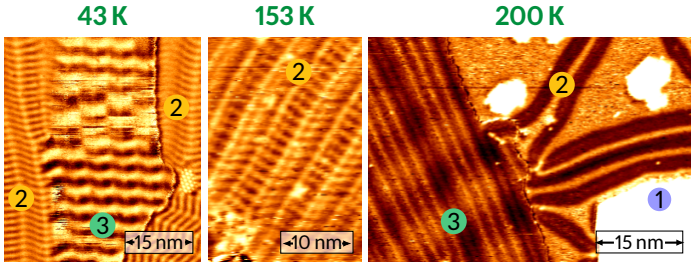

−700 mV, 1 nA −500 mV, 2 nA −700 mV, 2 nA, 0 T, Fe coated W tip

A. Finco *et al.* *Phys. Rev. Lett.* 119 (2017), 037202

Spin spirals at room temperature

8 K

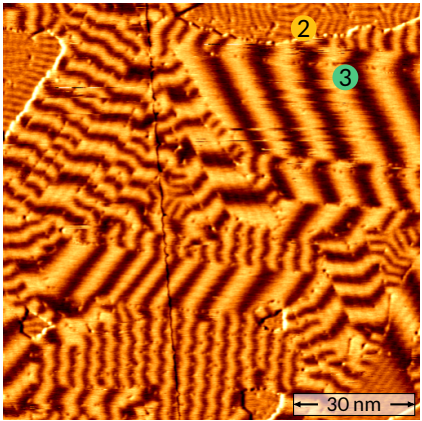

−700 mV, 1 nA, 0 T, Cr bulk tip

300 K

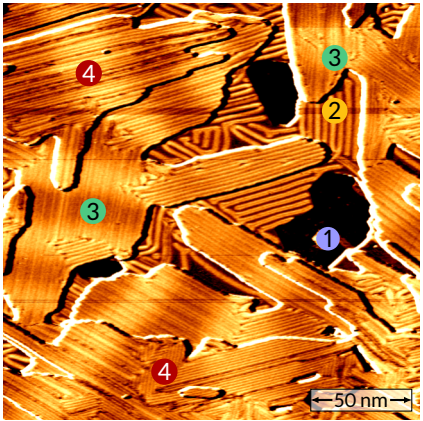

−500 mV, 3 nA, 0 T, Cr bulk tip

A. Finco *et al.* *Phys. Rev. Lett.* 119 (2017), 037202

Temperature dependence of the spiral period

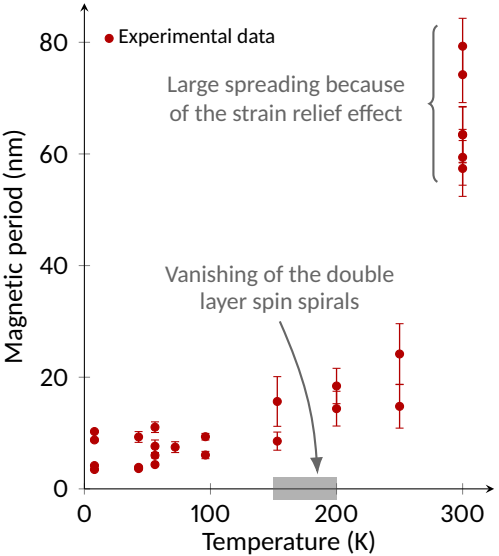

A. Finco *et al.* *Phys. Rev. Lett.* 119 (2017), 037202

Temperature dependence of the spiral period

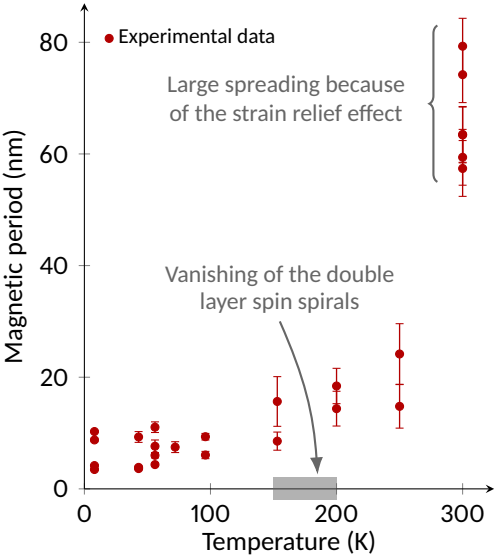

Model *(developed by Levente Rózsa)*

$$H = \frac{1}{2}\sum_{p,q,\langle i,j\rangle} J_{pq,ij}\,\vec{S}_{p,i}\cdot\vec{S}_{q,j} + \frac{1}{2}\sum_{p,\langle i,j\rangle}\vec{D}_{pp,ij}\cdot\left(\vec{S}_{p,i}\times\vec{S}_{p,j}\right)$$

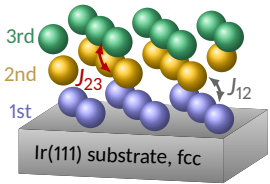

- No effective anisotropy
- Different *J* and *D* in the 3 layers
- Interlayer exchange coupling

The thermal fluctuations have a stronger effect on the 1st and 2nd layers
→ the magnetic state is imposed by the third layer at elevated temperatures.

A. Finco *et al.* *Phys. Rev. Lett.* 119 (2017), 037202

Temperature dependence of the spiral period

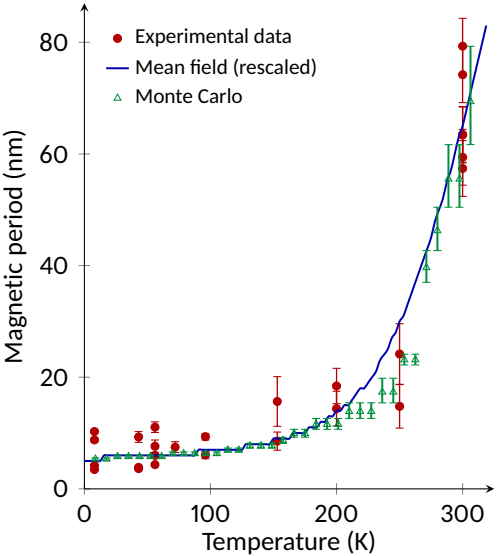

Model *(developed by Levente Rózsa)*

$$H = \frac{1}{2}\sum_{p,q,\langle i,j\rangle} J_{pq,ij}\,\vec{S}_{p,i}\cdot\vec{S}_{q,j} + \frac{1}{2}\sum_{p,\langle i,j\rangle}\vec{D}_{pp,ij}\cdot\left(\vec{S}_{p,i}\times\vec{S}_{p,j}\right)$$

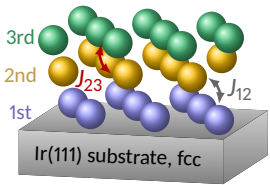

- No effective anisotropy
- Different *J* and *D* in the 3 layers
- Interlayer exchange coupling

The thermal fluctuations have a stronger effect on the 1st and 2nd layers
→ the magnetic state is imposed by the third layer at elevated temperatures.

A. Finco *et al.* *Phys. Rev. Lett.* 119 (2017), 037202

Summary

Pinning at the bridge lines in Ni/Fe/Ir(111)

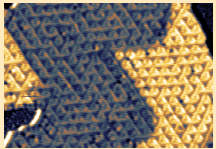

- Triangular pattern created by strain relief
- Domain walls following the long bridge lines

A.Finco, M. Perini *et al.*, in preparation

Tuning non-collinear magnetism in the Fe triple layer on Ir(111)

- Spin spiral period depending on epitaxial strain relief and temperature
- Skyrmions in external magnetic field, manipulated with electric field

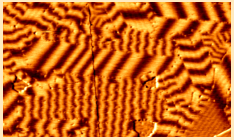

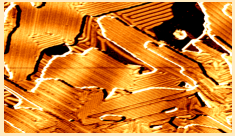

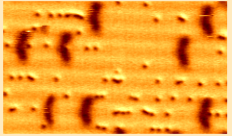

A. Finco *et al.* *Phys. Rev. B* 94 (2016), 214402
A. Finco *et al.* *Phys. Rev. Lett.* 119 (2017), 037202
P.-J. Hsu, A. Finco *et al.* *Nat. Nanotechnol.* 12 (2017), 123–126